Molecular Biology of the Cell
Vol. 16, 3620–3631, August 2005

Actin Filament Bundles in *Drosophila* Wing Hairs: Hairs and Bristles Use Different Strategies for Assembly

Gregory M. Guild, Patricia S. Connelly, Linda Ruggiero, Kelly A. Vranich, and Lewis G. Tilney

Department of Biology, University of Pennsylvania, Philadelphia, PA 19104-6018

Submitted March 10, 2005; Revised April 25, 2005; Accepted May 18, 2005
Monitoring Editor: Paul Matsudaira

Actin filament bundles can shape cellular extensions into dramatically different forms. We examined cytoskeleton formation during wing hair morphogenesis using both confocal and electron microscopy. Hairs elongate with linear kinetics (~1 μm/h) over the course of ~18 h. The resulting structure is vividly asymmetric and shaped like a rose thorn—elongated in the distal direction, curved in two dimensions with an oval base and a round tip. High-resolution analysis shows that the cytoskeleton forms from microvilli-like pimples that project actin filaments into the cytoplasm. These filaments become cross-linked into bundles by the sequential use of three cross-bridges: villin, forked and fascin. Genetic loss of each cross-bridge affects cell shape. Filament bundles associate together, with no lateral membrane attachments, into a cone of overlapping bundles that matures into an oval base by the asymmetric addition of bundles on the distal side. In contrast, the long bristle cell extension is supported by equally long (up to 400 μm) filament bundles assembled together by end-to-end grafting of shorter modules. Thus, bristle and hair cells use microvilli and cross-bridges to generate the common raw material of actin filament bundles but employ different strategies to assemble these into vastly different shapes.

INTRODUCTION

Cell function is intimately tied to cell shape and there is an abundance of cell shapes in multicellular eukaryotes. Cytoskeleton assembly differences using cross-bridged actin filaments can make huge differences in cell shape and as a consequence cell function. For example, bundling polarized actin filaments can give rise to rather stable structures like the microvilli present on the apical surface of intestinal epithelial cells, whereas nucleation with the Arp2/3 complex can yield the more dynamic lamellipodia seen in crawling cells.

The vast majority of the epithelial cells that cover insects elaborate cellular extensions. In *Drosophila*, a significant fraction of the thoracic cells form moderate (70 μm) or long (400 μm) bristles or chaetae that are innervated and play mechanosensory roles. In addition, a large percentage of wing blade cells build shorter (10–20 μm) extensions called hairs or trichomes that are not innervated and presumably play a passive role in directing airflow over the wing. Both bristles and hairs have a well-defined plane of asymmetry and as a consequence, cell extensions point in the same direction and extend from prescribed locations on the epithelial surface.

Over the last few years we have studied the formation of the thoracic bristle cytoskeleton. These cells sprout during metamorphosis and elongate over the course of ~18 h. Growth takes place at the bristle tip (Lees and Picken, 1944) and is driven by actin filament polymerization (Tilney *et al.*, 2000a). The actin bundles in bristle sprouts begin as microvilli (Tilney *et al.*, 2000b) and are cross-bridged into modular bundles 1–5 μm in length by at least two cross-linking proteins, forked and fascin (Tilney *et al.*, 1998, 2000b). These modules are then grafted together by end-to-end joining into stiff bundles (Guild *et al.*, 2003), which run longitudinally along the bristle shaft attached to the plasma membrane (Tilney *et al.*, 1996) and support the cell extension as well-spaced ribs. Bundles are tapered with the largest cross-sectional area of individual bundles at the base containing >500 filaments (Tilney *et al.*, 1996).

The wing is a relatively homogeneous tissue consisting of one-cell-layer-thick epithelium folded on itself. Most of the cells in this epithelium (there are ~30,000) elaborate a single distally pointing hair. These facts coupled with the flatness of the wing and the lack of cell divisions at the time of hair emergence (Mitchell *et al.*, 1983) makes this tissue an excellent system for both genetic and cell biological approaches. In fact, this system has proven to be an excellent model for studying planar cell polarity (e.g., Tree *et al.*, 2002). Like bristles, wing hairs also emerge and elongate during metamorphosis (Mitchell *et al.*, 1983; 1990; Fristrom and Fristrom, 1993; Wong and Adler, 1993; Turner and Adler, 1995, 1998). Elongating hairs contain high concentrations of F-actin when viewed by fluorescence microscopy (Fristrom and Fristrom, 1993; Wong and Adler, 1993; Eaton *et al.*, 1996), and mature hairs contain bundles of fibers when viewed in longitudinal sections (Mitchell *et al.*, 1983, 1990). Thus, both bristle and hair cells use actin filament bundles to generate cell shape.

There are a number of reasons to suggest that thoracic bristle and wing hair cells are homologous. Both cells differentiate in the epidermis during metamorphosis and exhibit planar cell polarity. Both cells construct an extension with a curved shape that protrudes toward the outside of the animal. Finally, both cells initiate elongation using actin

This article was published online ahead of print in *MBC in Press* (http://www.molbiolcell.org/cgi/doi/10.1091/mbc.E05–03–0185) on May 25, 2005.

Address correspondence to: Gregory M. Guild (gguild@sas.upenn.edu).

filaments derived from microvilli and use a common set of proteins—actin filaments and cross-bridges—to construct a cytoskeleton extension. These parallels make it easy to suggest that cytoskeletal homology is continuous from the molecular components right through the assembly process. However, these two cell types produce remarkably different structures that have very different functions. Bristles are long and cylindrical and serve an active antenna-like function, whereas hairs are short, shaped like a rose thorn, and have a noninnervated passive role. Here we show that bristle and hair cells use similar cytoskeletal components but *different* assembly strategies to accomplish this.

MATERIALS AND METHODS

Drosophila Stocks and Developmental Staging

The Oregon-R strain of *Drosophila melanogaster* was used as the wild type in these studies. The *singed* stock (sn^3), *forked* stock (f^{36a}), and *singed-forked* (sn^3 f^{36a}) double-mutant stock were maintained as viable homozygotes. Villin mutants were qua^1/qua^{6-396} transheterozygotes constructed from balanced stocks. A viable and fertile stock containing two copies of the wild-type *forked* gene and four transgenic copies (for a total of six copies per diploid female genome) was generously provided by Nancy Petersen (University of Wyoming, Laramie, WY; Petersen *et al.,* 1994). Elongating wing hairs were labeled in vivo using the GAL4/UAS system (Brand and Perrimon, 1993) by combining the third chromosome 71B GAL4 driver (Johnson *et al.,* 1995) with the second chromosome UAS-GFP-actin fusion of Verkhusha *et al.* (1999) generously provided by Jeff Axelrod (Stanford University) and Vladislav Verkhusha (Japan Science and Technology Corporation, Kyoto, Japan), respectively. Flies were maintained on standard cornmeal-molasses-yeast food at 25°C, 60–70% relative humidity, with a 12 h/12 h day/night cycle. Complete descriptions of genes and symbols can be found in Lindsley and Zimm (1992) and on FlyBase (Drysdale *et al.,* 2005). Developmental staging was as described previously (Tilney *et al.,* 2003).

Animals were staged from the point of puparium formation, an easily recognizable and brief stage lasting ~30 min at the beginning of metamorphosis (Bainbridge and Bownes, 1981). White prepupae were collected and placed on double-sided Scotch tape in a Petri dish and returned to the 25°C incubator. Times given are hours after white puparium formation at 25°C.

Wing Hair Measurements

Adult Wings. Wings from sexed animals were examined by scanning electron microscopy (SEM). Hair lengths were measured from digitized SEM images using the ImageJ (http://rsb.info.nih.gov/ij/) and Microsoft Excel applications (Redmond, WA). All measurements were confirmed by light microscopy of wings mounted in Gary's magic mountant (Lawrence *et al.,* 1986) under a coverslip and photographed with brightfield illumination using an Olympus BX50 compound microscope (Melville, NY) equipped with a DP12 digital camera.

Pupal Wings. Animals of the indicated ages (25°C) were removed from their pupal cases. Thoraces were dissected, fixed with formaldehyde (Tilney *et al.,* 2003), and stained with fluorescent phalloidin as described previously (Guild *et al.,* 2002). Wing hairs were imaged by confocal microscopy, measured, and analyzed as described above.

Real-time analysis of wing hair elongation was performed by time-lapse confocal microscopy (Guild *et al.,* 2002, 2003). Pupae expressing GFP-actin were dissected from their pupal cases at appropriate times and placed on their side in a chamber on a microscope slide defined by a silicone rubber isolator (Molecular Probes, Eugene, OR), covered with 1–2 μl of Halocarbon-56 oil (Halocarbon Products, River Edge, NJ) and a coverslip. Oxygen was streamed through chamber, and the animals were imaged using an Olympus Fluoview model BX50 confocal microscope. For each series, the same region of a wing disk was imaged periodically over a 6-h interval. The growing hairs were measured and analyzed as described above.

Antibody Staining

The procedures for dissection, fixation, antibody and phalloidin staining, and confocal microscopy were described previously (Guild *et al.,* 2002, 2003). During dissection, thoraces were split longitudinally and each half (with its associated wing bud) was stained with a different antibody to eliminate uncertainties about developmental age when staining patterns were compared. Mouse monoclonal antibodies directed against the quail protein (6B9, *Drosophila* villin) and the singed protein (sn7C, *Drosophila* fascin) were developed by Mahajan-Miklos and Cooley (1994) and Cant *et al.* (1994), respectively, and obtained from the Developmental Studies Hybridoma Bank developed under the auspices of the National Institute of Child Health and Human Development and maintained by the University of Iowa. The rabbit polyclonal antibody directed against the forked proteins was described previously (Guild *et al.,* 2003).

Electron Microscopy

Methods for fixation and processing of tissues for transmission electron microscopy (Tilney *et al.,* 1998) and for SEM (Tilney *et al.,* 2004) have been described.

RESULTS

Adult Wing Hairs

To determine the time course of hair elongation and to couple this information with the appearance of actin binding proteins and the characteristics of the cytoskeleton as determined by electron microscopy, it is essential at the onset to measure final hair length and to characterize the shape of the adult hairs.

Although most hairs point in the same direction, the orientation of hairs in different patches can vary by as much as 30°. As one looks down on the hairs with a scanning electron microscope one can see slight differences in hair lengths in different wing regions. To compare different genotypes we measured hair length by sampling eight easily recognizable regions of the wing (Figure 1A, asterisks) neglecting the hairs that lie over the veins because these tend to be shorter and more poorly oriented. Even in a single field, hairs can vary in length from 16 to 18 μm or as much as 12% (Figure 1B). Not surprisingly, there are sex differences in average hair lengths (see below).

Time Course for Elongation

The literature for the time course for hair elongation is controversial. For example, earlier investigations indicated that hairs elongate rapidly and reach their mature length in 33–35 h pupae (Mitchell *et al.,* 1983), whereas later work indicates that elongation occurs during a 10-h period (in 36–46 h pupae), but mature lengths are only reached in adults (Turner and Adler, 1995; 1998).

Because of such wide discrepancies, we reexamined the time course for elongation. This is particularly important for future studies when one tries to integrate the timing of planar cell polarity gene action and the timing of these cell shape changes. We studied cell elongation in two ways. First we examined wings fixed at increasing intervals after pupation and visualized hairs by staining with fluorescent phalloidin (Figure 2A). We find hairs begin to emerge at 30 h after pupariation and reach their mature length in 47-h pupae. Second, we measured hair elongation in real time by imaging hairs labeled with GFP-actin. Because the same portion of the cultured wing was examined repeatedly, we only measured the rates of elongation for 7 h on any individual wing. To see the entire time course then requires two sets of wings, one removed from 32-h pupae (Figure 2B) and the other from 40-h pupae (unpublished data). Both sets of observations show that hair elongation takes ~17 h and that the rate of elongation is linear at 0.9–1.0 μm/h. This is in contrast to thoracic bristle elongation where microchaetes (70 μm) and macrochaetes (400 μm) elongate with exponential kinetics at rates centering around 4 and 25 μm/h, respectively (Tilney *et al.,* 2000a).

Morphology of Adult Hairs

Hairs like bristles taper and curve. However, hairs are not cone shaped like bristles but rather resemble rose thorns, nearly round at their tips, and as one progresses toward the base, the lateral surfaces are larger than the superior or inferior surfaces. This morphology can be seen by slicing the

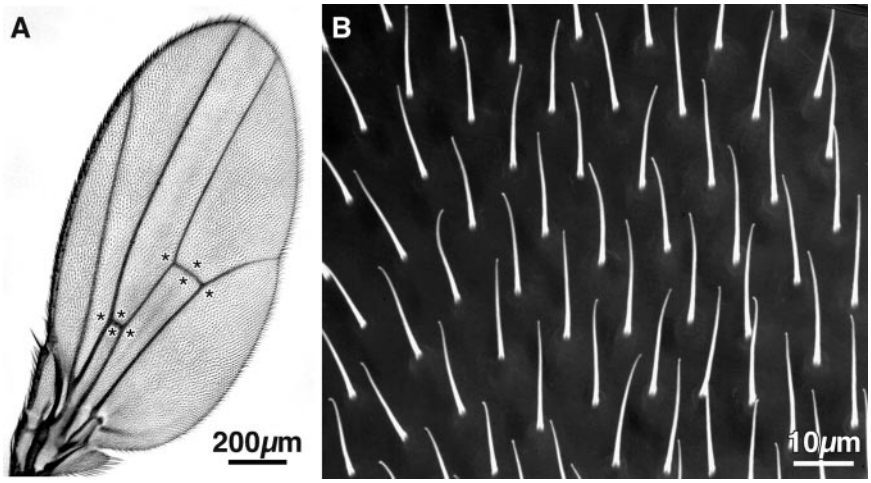

Figure 1. (A) Light micrograph of the wing from a wild-type adult *Drosophila*. The asterisks indicate the regions sampled to measure hair length. (B) Low magnification SEM micrograph of a portion of a wild-type wing showing the hairs. Note that although the hairs are all oriented in approximately the same direction (i.e., toward the tip of the wing) the ends of the hairs are frequently bent in one direction or the other.

mature wing in half and positioning it on the stub for the SEM cut edge up so that an individual hair can be photographed along its superior surface, and then by tilting it 90°, the same hair can then be photographed on its lateral surface. Such images (Figure 3, A and B) reveal that the base is indeed like a rose thorn (Figure 3C), but also that the cur-

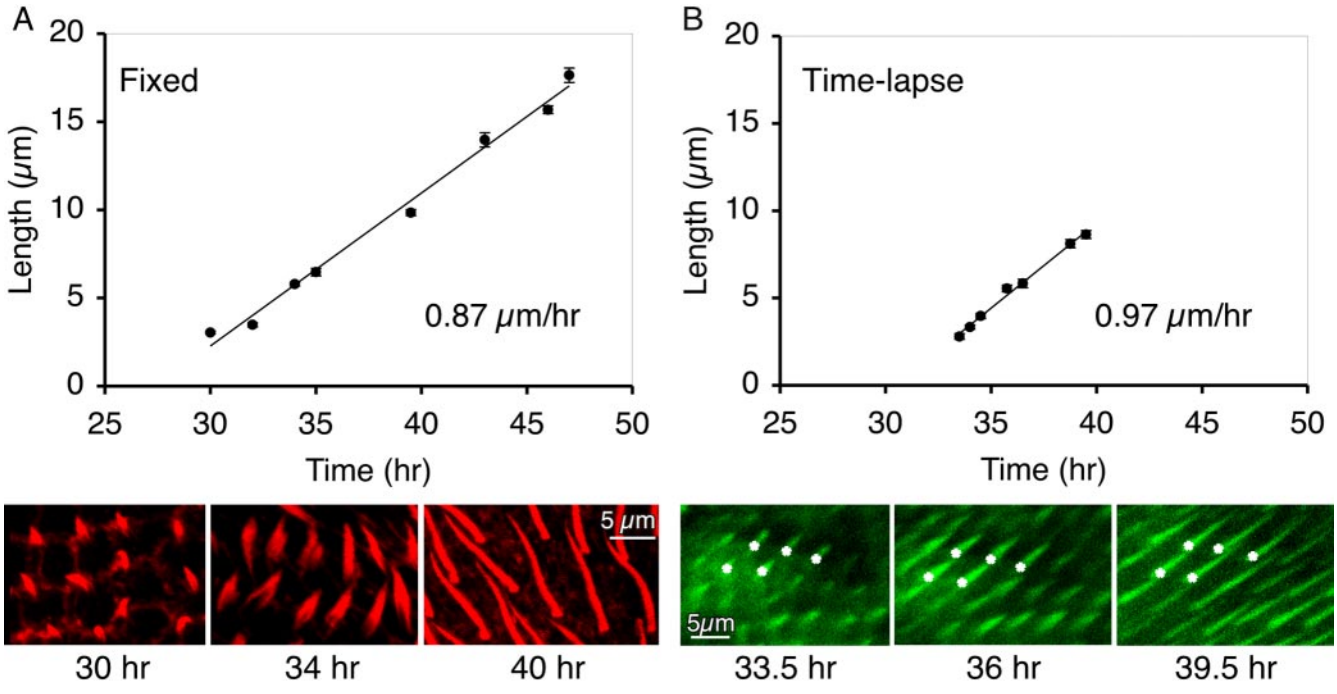

Figure 2. Kinetics of wild-type wing hair elongation. (A) Fixed hairs. White prepupae (t = 0) were collected and allowed to age at 25°C for the indicated times. For each time point, wing hairs stained with fluorescent phalloidin were imaged and measured. A total of 742 hairs from 33 animals were measured. Bars, SE of the mean for each measurement. A linear trend line fitted to the data indicates that hairs elongate at a rate of 0.87 μm/h. Examples of phalloidin-stained wing hairs from 30-h (left), 34-h (middle), and 40-h (right) animals are shown at the same magnification below. The 34-h hairs often show distinct actin bundles at the base of the hair. (B) Time-lapse. White prepupae (t = 0) were collected, aged for 33 h (25°C), removed from their pupal cases, allowed to develop in a chamber (24–26°C) on the microscope stage, and imaged over the course of 6 h. The same 10 hairs from one wing were measured during this time course and plotted. Bars, SE of the mean for each measurement. A linear trend line fitted to the data indicates these hairs elongated at a rate of 0.97 μm/h. Examples of GFP-expressing wing hairs from 33.5-h (left), 36-h (middle), and 39.5-h (right) animals are shown at the same magnification below. For reference, the same five elongating hairs are marked with asterisks. A total of 40 hairs from four animals in four independent experiments gave similar growth rates (0.88 ± 0.09 μm). All images (in A and B) are shown at the same magnification. Bar, 5 μm.

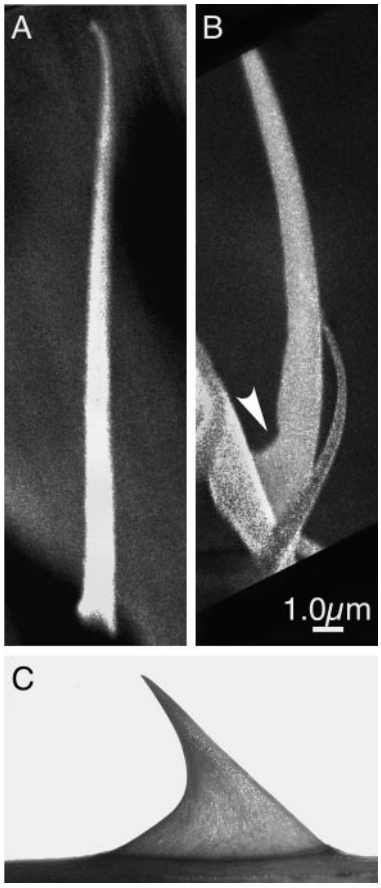

Figure 3. Wing hair shape. (A) SEM of a wild-type hair as one looks down on it from above. (B) The wing was then tilted 90° and rotated and the same hair was viewed from the side. (C) Rose thorn in profile. Thus each hair resembles a rose thorn in three dimensions, a rose thorn that is thicker at the base (arrowhead in B) than at the tip. The tip is missing in B. These images show that the hair must have an oval profile in section.

Figure 4. Thin section through a portion of the surface of a wild-type 33-h pupal wing. Two wing hairs are present near the top of the micrograph and grazing sections through epithelial cells are found at the center and bottom of the figure. The arrowheads point to short protuberances of the plasma membrane, which we refer to in the text as pimples.

vature is planar not three-dimensional. From these same images and from phase microscopy the surface of the hairs sometimes appears fluted, although unlike bristles the fluting is subtle and not at precise intervals.

The Fine Structure of Developing Wing Hairs

We used electron microscopy of thin sections to analyze the detailed structure of hairs from pupae of increasing age.

33-h Pupae All along the surface of the epithelial cells are pimples, tiny projections of the cortical cytoplasm (Figure 4). Characteristically there is some electron-dense material lining the cytoplasmic surface of these projections and in some cases filaments can be seen extending a few nanometers into the cytoplasm. We previously concluded that these pimples were precursors to microvilli formation (Tilney *et al.*, 2004).

Hairs begin to sprout from the distal vertex of the epithelial cells. These sprouts are broad (Figure 2) and contain a number of pimples (Figure 4) but unlike the pimples, on the rest of the surface of the epithelial cells the pimples on the sprout have bundles of actin filaments extending into the cytoplasm often for distances of 1 μm or more (Figure 5). Although the filaments in these groups lie roughly parallel to one another there is no precise order to their packing in longitudinal or cross sections, due to cross-bridges (Figure 5B)—features we find in slightly older pupae (see below).

In hairs that have elongated a bit more the sprouts become thinner and taper toward the tip (Figure 6A). Actin filaments extend from the pimples located at the tapered tip (Figure 6, A and C) as well as from pimples located along the lateral surfaces of these projections (Figure 6A). Generally these filaments are in loose bundles lying near the plasma membrane limiting the hair (Figure 6D). The filaments in these bundles are not precisely packed but are separated from each other by variable distances.

At or near the bases of these sprouting hairs are commonly split (Figure 6B) with pimple-like protuberances (arrow Figure 6A), with actin filaments extending further basally from them. We presume that these images represent stages in the conversion of a symmetrical cone-shaped sprout into the rose thorn appearance seen in fully mature hairs. This seems to be accomplished by the selective activation of pimples to form filament bundles on only one margin of the base of the hair.

We should also mention that unlike the situation in elongating bristles from pupae of comparable age, the hair ex-

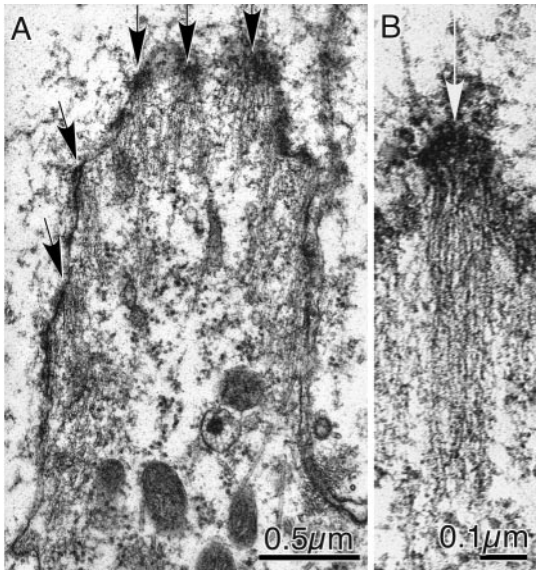

Figure 5. Thin sections through newly emerging wing hairs from a wild-type 33-h pupa. (A) The arrows indicate the pimples seen in Figure 4 at higher magnification. Of interest is that a bundle of filaments extend from each pimple into the cytoplasm. (B) A pimple, indicated by the white arrow, and its associated bundle of filaments that originate from electron dense material attached to the cytoplasmic surface of the plasma membrane. The filaments in the bundle are not hexagonally packed.

oskeleton begins to form even in pupae of this age (Figure 6, C and D). What we see are small spots or segments of exoskeletal material attached to the plasma membrane. These spots, which appear nearly round in grazing section, consist of two dense parallel lines separated by 100 Å (arrowheads, Figure 6, C and D) in cross section. These spots will fuse together in older pupae to form the outer extracellular layer of exoskeleton (see below). A spot of this extracellular material covers the bristle tip (Figure 6C). In favorable sections the extracellular spots are seen attached to the plasma membrane by tiny periodic connections. At these junction points the plasma membrane itself appears thicker due to the accumulation of material to its cytoplasmic surface.

36-h Pupae By this stage we find large and often dense populations of actin filaments within the hair proper (Figure 7A). Most of the filaments are not clustered together but run for considerable distances down the hair shaft. In a *few* cases, clusters of filaments are present near the plasma membrane (Figure 8C). In these cases a faint 12-nm transverse periodicity is visible. Except at the tip the microtubules are sometimes present within the deeper shaft cytoplasm (Figure 7C). Immediately lateral to the base of hairs we frequently find short microvilli (Figure 7A, arrowhead) with a bundle of actin filaments extending into the cortical cytoplasm. As mentioned before we presume that these will result in the widening of the hair base. However, as seen in the transverse sections illustrated in Figure 7, D–F, widening of the hairs, which should produce an oval base, does not occur at this stage.

The exoskeleton surrounding the hairs at this stage is more prominent than in the younger pupae. Many of the tiny exoskeletal segments have fused together to form longer plates (Figure 7C). Between these longer stretches of exoskeletal material the surface of the hair not enclosed by exoskeletal material bulges outwards as if the exoskeleton acts to reduce surface irregularities (Figure 7C). Sections through the tip of the hairs reveal a cap of exoskeleton material covering the tip (Figure 7B) as was seen in earlier pupae. As one moves basally the exoskeleton becomes intermittent although segments of it are often joined together. Just beyond the tip, which is characterized by the exoskeletal cap and the fact that actin filaments terminate on the plasma membrane at the exact tip, we often see a tiny ring of exoskeleton that does not contain cytoplasm or a section through plasma membrane (Figure 7B). We interpret this ring as being a tiny protrusion extending from the tip of the elongating hair.

40-h Pupae By 40 h the fine structure of the hairs begins to resemble that of the fully elongated hairs. The actin filaments within the hairs cluster together forming, for the first time, discrete albeit small bundles (Figure 8A). These bundles terminate at positions along the plasma membrane as one moves in a longitudinal section toward the tip. Examination of some of these bundles in longitudinal section reveals 12-nm periodic cross-striping (Figure 8C) reminiscent of the 12-nm period in bristles caused by the presence of the cross-bridge fascin (Tilney *et al.*, 1995). In transverse section we see that the filaments in the bundle are often hexagonally packed (Figures 8B and 9) as one would predict from the 12-nm period (Tilney *et al.*, 1995) but unlike the bristles the size and shape of the bundles is very small and irregular.

Transverse sections through the hairs near their base show that the hair is not round as they are near their tip but instead are oval (Figure 9). Thus by this stage each hair has the rose thorn–shape characteristic of mature hairs. Within the cytoplasm of these oval basal sections one sees that there are more actin filament bundles than at the tip and that they are spaced laterally throughout the oval bases. This feature can be best appreciated by examining a mutant that overexpresses the forked gene (Figure 9) and accordingly increases the degree of cross-bridging by fascin (Tilney *et al.*, 1998). Thus at this stage a round hair is being converted to a rose thorn shaped structure. The exoskeleton has become more prominent because the small spots of exoskeleton seen in younger pupal hairs have increasingly fused together to form in some cases a continuous layer (Figures 8 and 9). In some cases there still are discontinuities that give a scalloped appearance to the exoskeleton (Figure 8A).

46-h Pupae By this stage the exoskeleton is continuous and without gaps. Interior to the two dense lines, characteristics of the surface of the exoskeleton when viewed in thin section, is a thin layer of amorphous material (Figure 10) that will gradually increase in thickness as the pupa develops further. What has changed by this stage is that when sections are cut through the base of the hair we find that the cytoplasm together with its enclosing plasma membrane has pulled away from the exoskeleton (Figure 10B). This separation of the cell from the exoskeleton is likely to be the result of poor fixation or embedding. However, because these separations are not present in younger pupae, this is worth noting.

In our transverse sections near the base of the hair as mentioned before the overall shape of each hair is oval yet sections near the tip are round, again reinforcing the fact that the actin filaments are not only clustered into discrete bundles but also the filaments within each cluster are hexagonally packed. Where these clusters terminate (near the

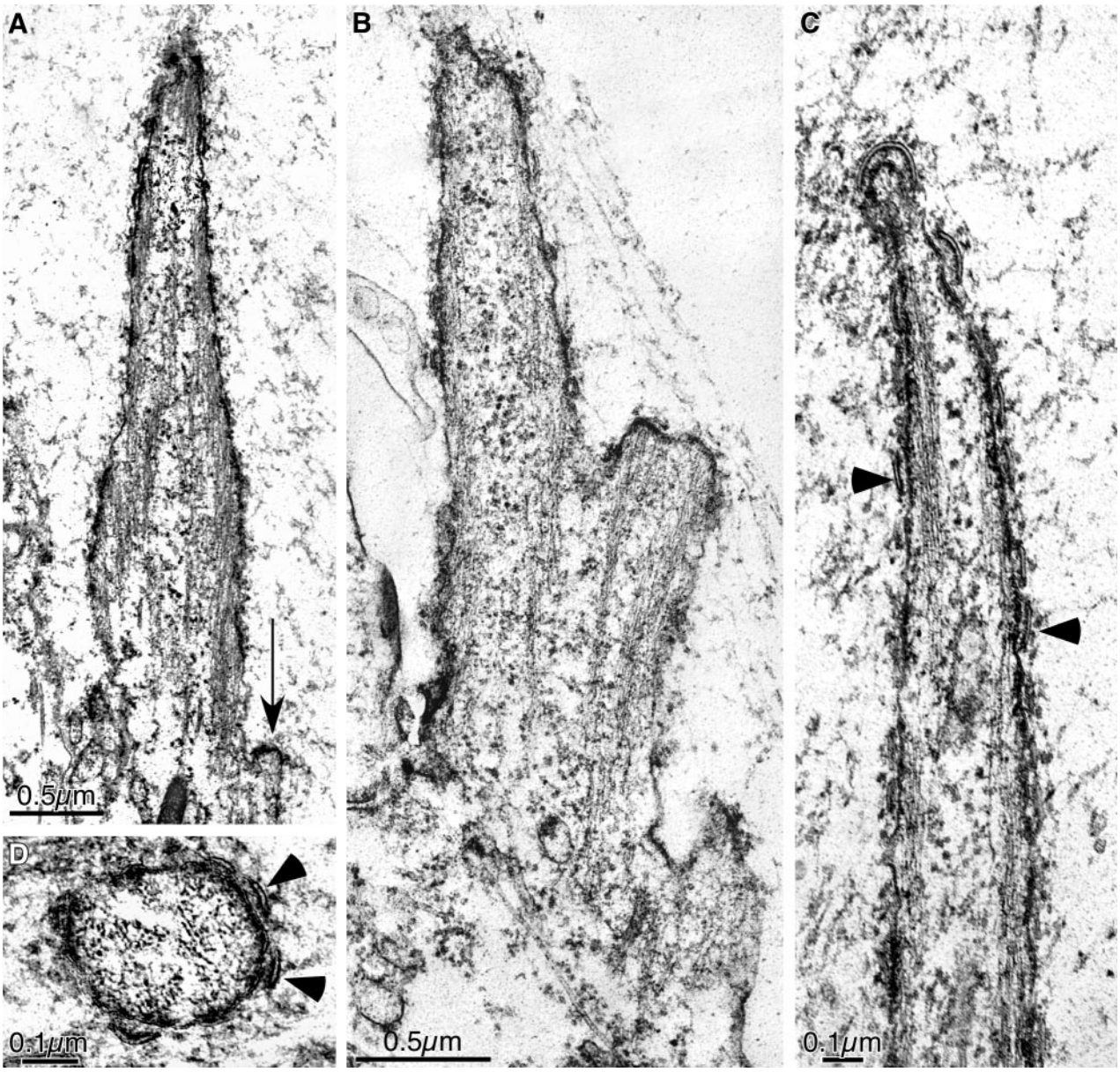

Figure 6. Thin sections through a variety of newly erupted wing hairs from wild-type 33-h pupae. Note that in all cases the hairs taper. (A) Bundles of actin filaments emanating from small densities on the plasma membrane are present along the surface and within the cytoplasm proper of the hair. The arrow indicates a pimple at the base of the hair from which actin filaments extend basally. (B) A branched hair. Bundles of actin filaments extend basally from the plasma membrane at the tips of the two branches. (C) The arrowheads point to small extracellular discs. The curved disk at the tip of this hair will eventually fuse together with those along the lateral surface to form the cuticle. (D) Transverse section through a hair. Within the cytoplasm are clusters of dots, which are the actin filaments cut in transverse section. These filaments are not well ordered. As in C the arrowheads point to cuticular discs.

tip or along the shaft), they do so into small densities attached to the limiting plasma membrane (arrows Figure 11A).

55-h Pupae By 55 h the apical surface of the epithelial cells have changed their shape in a new way. Each hair extends from the center of a platform, or pedicel first described by Mitchell *et al.* (1983). Just beneath the plasma membrane at the surface of the pedicel is an abundant population or meshwork of actin filaments (arrows in Figure 11A). The filaments appear oriented in all directions within this meshwork. The filament bundles have increased in diameter (Figure 11B) and clearly show the 12-nm period induced by fascin cross-bridging.

The exoskeleton is further developed by this stage because of an increase in amorphous material between the plasma membrane of the hair and the two dense lines characteristic if the surface of the exoskeleton (Figure 11B).

Cross-bridges That Connect the Actin Filaments in Hairs Accumulate in Sequence

To determine when the cross-bridges appear in hair shaft cytoplasm we stained developing wings with antibodies to villin, fascin, and the forked proteins (Figure 12). In 30-h

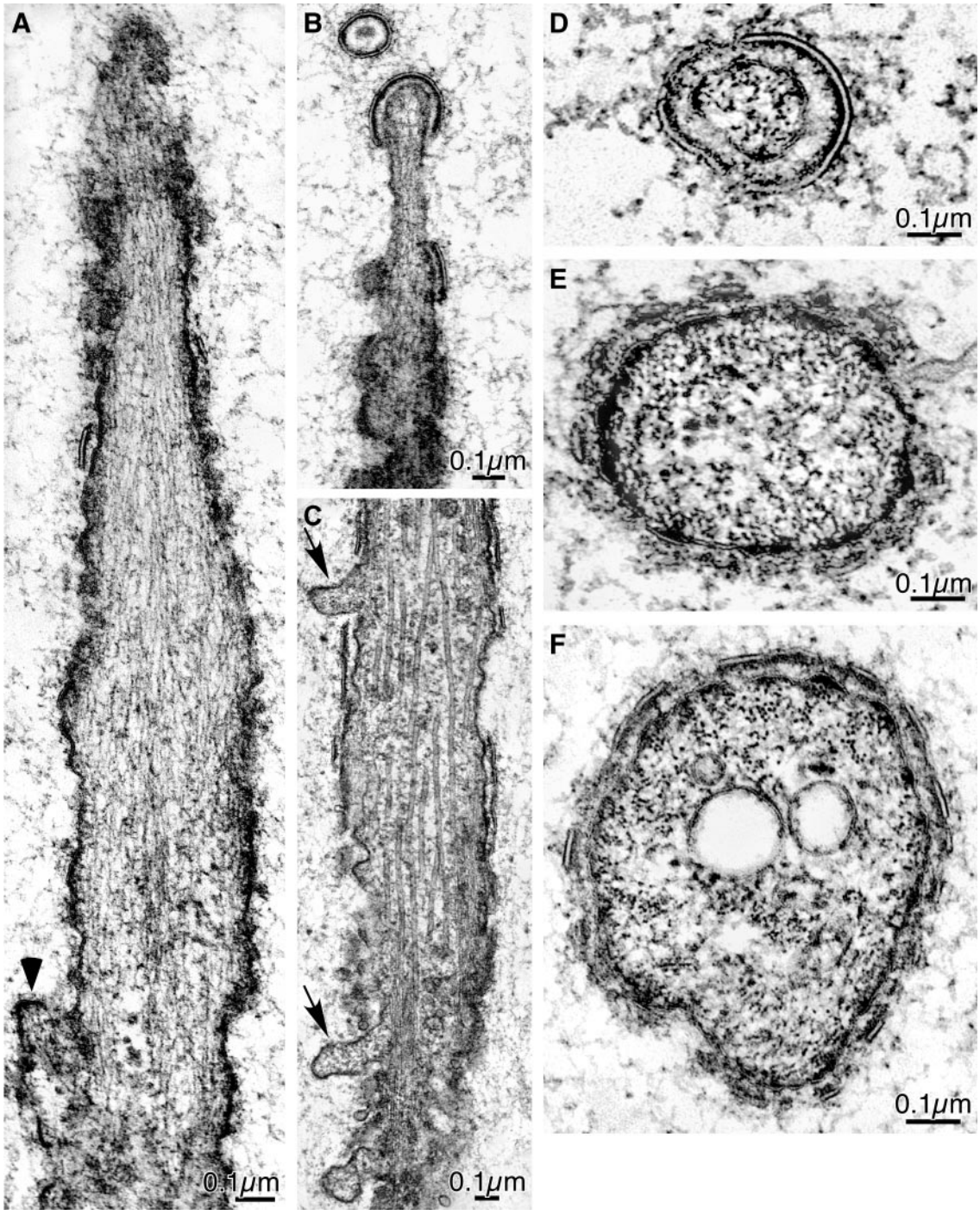

Figure 7. Thin sections through hairs from 36-h wild-type pupal wings. (A) The cytoplasm of the hairs is filled with actin filaments at this stage. The arrowhead points to a pimple at the base of the hair that has actin filaments attached to its cytoplasmic surface. (B) Thin section through the tip of a hair. Actin filaments extend to the tip, which is enclosed by a cuticular cap. (C) Thin section through the shaft. Of interest is that extending from the surface of the shaft are blebs of cytoplasm indicated by the arrows. Between the blebs are segments of cuticle. Microtubules are present within its shaft. Transverse sections through hairs: near the tip (D), midway down the shaft (E), and near the base (F). Bundles of actin filaments that in section appear as clusters of dense dots. The cuticle is nearly complete at the tip (D) but discontinuous near the base (F).

pupae villin is present in the hair shaft but forked is absent. By 34 h the amount of villin has increased dramatically but forked and fascin are not present. By 40 h villin is virtually absent but forked has increased dramatically brightly staining the hair shaft. Fascin is also present. We conclude that villin is likely to be responsible for clustering the filaments early in hair morphogenesis but disappears as the forked and fascin cross-bridges appear. These newly arrived cross-

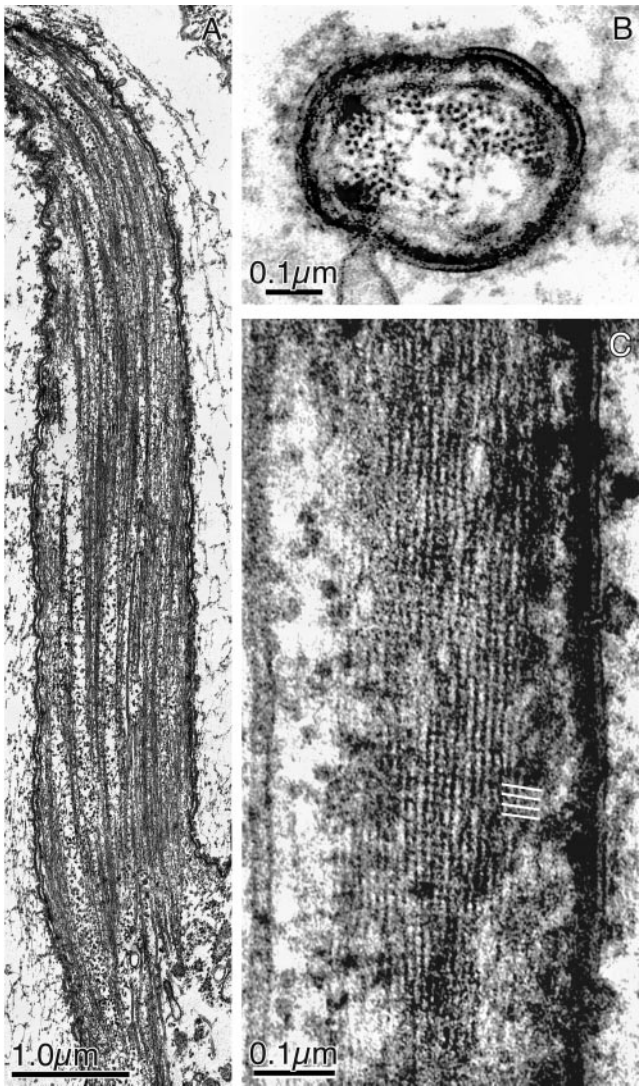

Figure 8. Thin sections through wing hairs of a 36-h wild-type pupa. These sections are unusual for this time of development. In these micrographs the actin filaments cluster closely together. In transverse section (B) the filaments in the clusters are hexagonally packed. In a favorable longitudinal section (C) 12-nm horizontal stripes as indicated by the white lines are present on the clusters. Our earlier studies in bristles show that this 12-nm striping is due to the fascin cross-bridge.

bridges then induce the formation of discrete filament bundles that overlap one another along the hair extension. By 48 h fascin remains but both forked and villin are absent.

Cross-bridging Proteins Are Important Determinants of Hair Length and Morphology

In Figure 13 we compare the length of wild-type hairs with those of four mutants. One of the mutants lacked the forked cross-bridge (*forked* mutant), another lacked fascin (*singed* mutant), a third lacks both forked and fascin (*forked-singed* mutant), and the fourth showed a severe reduction in villin (*quail* mutant). The first three show a reduction of 12–14% in hair length. The fourth mutant, a mutant that has a reduction in villin (*quail* mutant) has bristles that are 23% longer that the wild type. A *t*-test was used to compare mutant hair

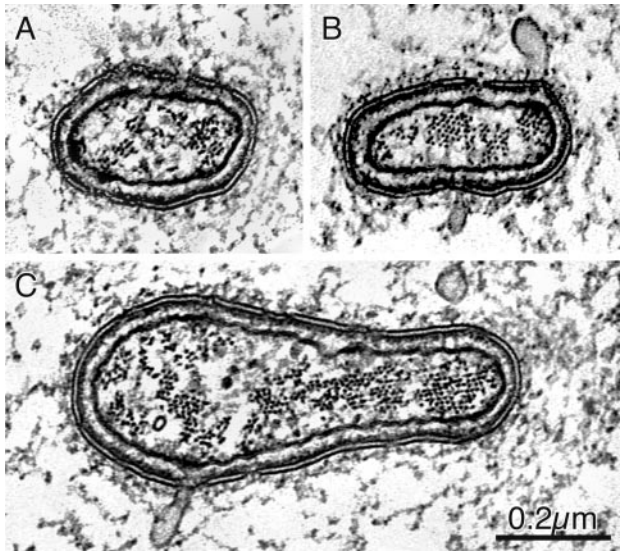

Figure 9. Thin transverse sections through wing hairs from 41-h animals overexpressing the forked proteins. The cut is near the tip (A), midway down the shaft (B), and near the base (C). Note that by this stage the base is oval in profile. Within each section the hexagonally packed dots are clusters of actin filaments cut in transverse section. Of interest is that as one progresses from the tip to the base the number of clusters increase. Most clusters lie free in the cytoplasm, not membrane associated. The cuticle is continuous around the surface of the hair.

lengths with that of the wild type. All comparisons (except the *quail* females) show a difference significant to the 0.0005 level. The increased length of hairs lacking villin is puzzling.

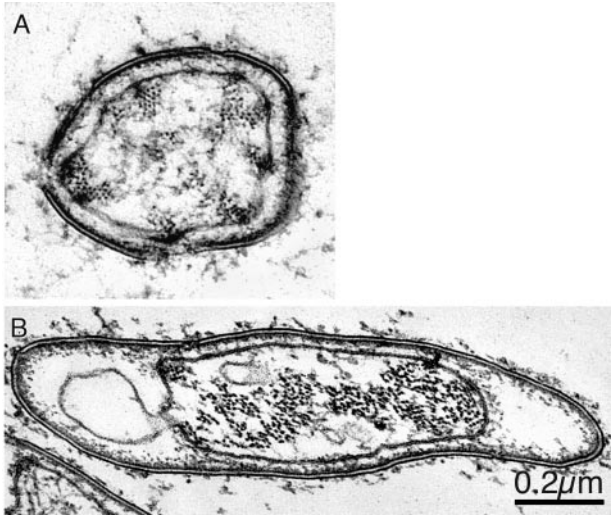

Figure 10. Transverse thin sections through wing hairs from 46-h wild-type pupal wings. (A) Tip. Of interest is that the bundles of hexagonally packed actin filaments at the tip, which at this stage is nearly round, are all located close to the plasma membrane as if connected to it. There is some electron-dense material attached to the cytoplasmic surface of the plasma membrane of these "connection" sites. (B) Base. In contrast to A, at the base of the hair the actin bundles are all cytoplasmic not membrane associated. Note that in thin section the hair base is oval, and the plasma membrane is not connected to the cuticle at the edges.

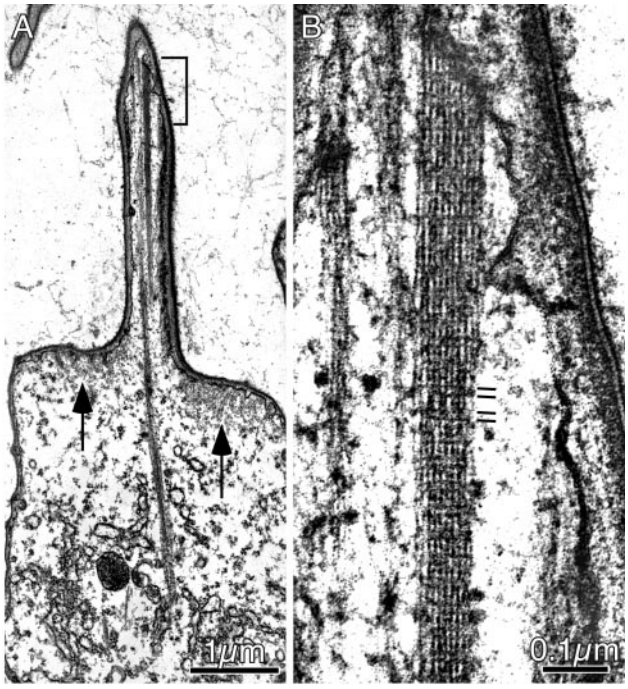

Figure 11. Transverse thin sections through 55-h wild-type pupal epithelial cell. (A) By this stage the apical surface of each epithelial cell forms a pedicel from which the hair extends. The pedicel is reinforced with a meshwork of actin filaments (arrows). A portion of the hair (bracket) is illustrated at higher magnification in B. Each bundle of actin filaments extends from the same electron-dense material attached to the cytoplasmic surface of the plasma membrane. The filaments are closely packed and show a 12-nm horizontal striping (see dark lines), indicative of cross-bridging by fascin.

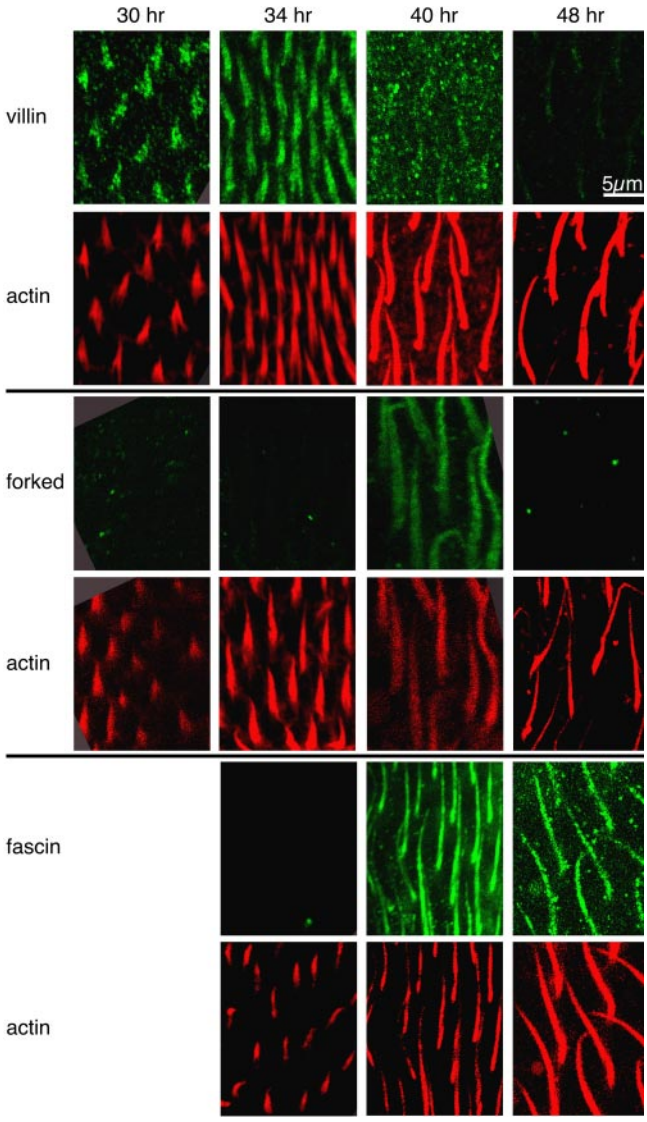

Figure 12. Sequential accumulation of actin filament cross-bridges during hair morphogenesis. Confocal images of wild-type wing hairs fixed and stained at different times during development (columns). Hairs were stained with Texas Red phalloidin (red) and antibody (green) directed against *Drosophila* villin (top section), forked (middle section), or fascin (bottom section). Of interest is that these cross-bridges appear sequentially. Villin is present in early pupae, whereas forked appears at 40 h, and fascin is present at 40 h and beyond. Equally interesting is that villin is essentially absent after 34 h and forked disappears after 40 h, but fascin remains at least through 48 h. Bar, 5 μm.

Perhaps cross-bridging of adjacent filaments in the clusters emanating from pimples stabilizes the filaments sufficiently so that there is a slight depletion of the actin monomer pool, sufficiently so that newly assembling filaments fail to assemble to a longer length, a feature that would influence total hair length. Thus if villin is absent the hair could grow longer.

Figure 13 also compares the morphology of the mutant and wild-type hairs as seen by SEM. All are presented at the same magnification from the same area of the wing and are printed in the same orientation. In the *forked*, *singed*, and *forked-singed* mutants the overall orientation of the hairs was similar to the wild type—they primarily extend toward the distal margin of the wing—but increased variation in orientation is present in these mutants. This is particularly noticeable in the *singed* mutants where 30–40° variations in adjacent hairs are common (unpublished data). But what is especially true in the *singed* mutants is that the hairs twist. The handedness of the twist is not constant and in fact some twist in one direction and then in the other. The *singed-forked* and the *forked* mutant hairs seem to be less rigid than the wild type and sometimes appear to lie on the surface of the wing. In contrast, the mutant lacking villin (*quail*) is curved and oriented like the wild type. What is particularly striking is that the mutant hairs like the wild type are thorn shaped in profile, which means that sections of hairs cut near the base present similar overall profiles.

So far we have only cut thin sections through *singed* mutant wings. Because this mutant lacks the fascin cross-bridge, we expected that the actin filaments in bundles would not be hexagonally packed, a fact established for the actin bundles in bristles of *singed* mutants (Tilney *et al.*, 1995, 1998). Although we found this to be true, what is even more striking is that few bundles are present in our transverse or longitudinal sections through *singed* hairs. Rather the actin filaments are present in an almost diffuse cortical layer (unpublished data).

DISCUSSION

We began this study with the preconception that the actin cytoskeleton in *Drosophila* bristle and hair cells were very

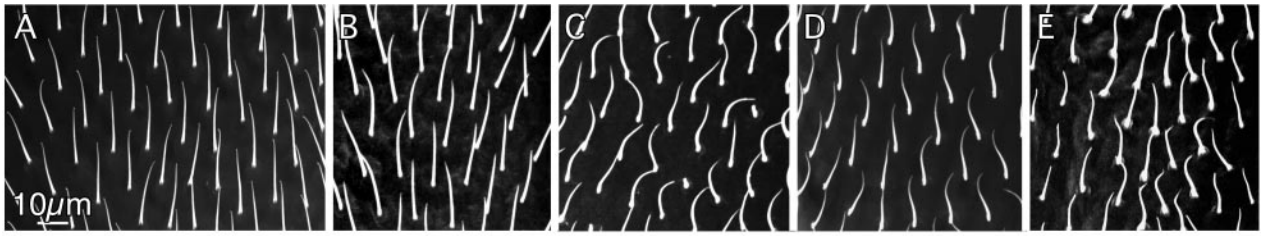

SEM measurements of wing hair lengths (μm)

	Wild-type	*quail*	*forked*	*singed*	*forked-singed*
male	16.51±0.11 (580)	20.39±0.14 (311)	14.60±0.08 (587)	14.51±0.08 (446)	14.15±0.12 (256)
female	15.85±0.09 (532)	15.78±0.21 (137)	14.67±0.08 (559)	12.47±0.09 (440)	14.41±0.14 (310)

Figure 13. (A–E) SEM micrographs of portions of adult wings showing the hairs in the wild-type and four mutants that affect cross-bridging. Below these micrographs are our measurements of hair lengths in male and female wings for the wild-type and mutants. Of interest is that the *forked*, *singed,* and *forked-singed* hairs are all shorter than the wild-type and frequently curved. In contrast, *quail* hairs (lacking villin) are longer than the wild-type, at least in males.

similar in structure. We anticipated that our study of hair morphogenesis would be simplified because we could make use of our knowledge of the bristle cytoskeleton (see *Introduction*). But what we found when we compare bristle and hair morphogenesis in detail is that although similarities exist, the differences between the two are profound. In fact, these differences make us cognizant that the elongation process is quite different in the two cells even though they utilize many of the same proteins. Accordingly, different assembly strategies lead to different cell shapes, which in turn relate to different functions.

Actin Cytoskeleton Assembly Dictates Cell Form

Pimples are involved in initiating the assembly of actin filaments that in turn are responsible for the elongation of the tip of the cell extension in both hairs and bristles (Tilney *et al.,* 2004; this report). However, in hairs only those pimples located on the distal vertex of the epithelial cell are activated, whereas all the pimples at the tip of a bristle process are activated. In addition, at the base of newly emerging hairs and specifically on the side of the hair nearest the distal vertex of the cell, new pimples must form and/or be activated in order to build the rose thorn shape. Thus hairs must receive at least one signal that dictates where the hair forms on the cell surface and another that activates pimples asymmetrically. Hair cells clearly exhibit planar cell polarity (PCP) that ultimately results in a subcellular asymmetry that is regulated by both inter- and intracellular components (reviewed in Adler, 2002; Lawrence *et al.,* 2002; Tree *et al.,* 2002). It seems likely that the asymmetric activation of hair cell pimples represents a readout of this subcellular asymmetry.

Interestingly, the actin bundles in bristles are large in cross-sectional area on the inferior surface and small or in some cases absent on the superior surface (Tilney *et al.,* 1995). Thus there is a correspondence in bristles and hairs with respect to thicker (bristles) and more (hairs) bundles on their inferior surfaces. So like hairs, there may also be an asymmetry in pimple activation on bristles during bundle formation. Because PCP pathways also regulate bristles, pimple activation may represent a common readout in both cell types.

Cytoskeleton structure is very different in the two cell types. In bristles tiny bundles are pulled together near the bristle tip and become short bundles or modules 1–5 μm in length. These newly formed modules are then grafted to bundles that lie beneath them longitudinally to produce the membrane associated "ribs" that encase and presumably support the bristle. Bundles are not found in the bristle cytoplasm proper. In hairs the tiny pimple-derived bundles overlap the bundles beneath them such that there are few bundles at the tip and larger and larger numbers of parallel overlapping bundles as one moves toward the bristle base. Although these bundles are attached to the plasma membrane at their tips most do not bind to the membrane on their lateral surfaces but instead fill up the cytoplasm of each hair. In hairs then there are no riblike membrane associated modules but instead overlapping cytoplasmic bundles.

These major differences in the form of the actin bundles in these two types of extensions must be due in part to the observed differences in cross-bridging. In bristles the forked proteins are present very early in bristle elongation and facilitate the subsequent entry of fascin into the bundles (Tilney *et al.,* 1998). In contrast, the villin cross-bridge appears early in hairs but is not present in bristles. It presumably functions in hair morphogenesis by clustering the filaments emanating from the pimples into loose bundles at early stages in bundle formation and bundle clustering. Villin then largely disappears from the hairs and is replaced by the forked proteins and fascin. Maximal cross-bridging by fascin becomes progressively more apparent in older hairs and is accomplished in the absence of the forked proteins. This is unlike fascin cross-bridging in bristles where the forked proteins can be visualized by antibody staining in mature bundles (Tilney *et al.,* 2000b; our unpublished data).

Of course other factors influence the stability of the respective extensions. One of the most important is the leathery chitinous layer that surrounds and is attached to the plasma membrane of both hairs and bristles. We demonstrate here that this layer is formed by the fusion of small units into a continuous cover, something that Mitchell *et al.* (1983) also documented. From our thin sections, although they only present us with a window into the process of cuticle secretion, it appears that the exoskeleton is continuous in 40-h pupae, a stage where the hairs have only elongated to two-thirds of their mature length. Before that time blebs of bulbous material extend outward between segments of exoskeleton (Figure 7B). From these images we conclude that the exoskeleton functions at least in part by ensuring that the surface of the hair is smooth. Presumably it also stabilizes this extension. What is interesting is that the exoskeleton in hairs appears complete in 40-h pupae right up to their tips yet in bristles the exoskeleton is not complete for another 8 h. This is particularly apparent in sections cut near the bristle tips, where gaps in the exoskeleton exist (unpublished observations).

Form Dictates Function

Hairs and bristles elaborate cellular extensions that differ in orientation, rigidity, and shape. On the wing, hairs must all point in the same direction, extend from the same position on the epithelial cells, and exhibit rigidity—all to avoid overlap, presumably for aerodynamic reasons. Bristles on the other hand are extensions of the entire apical surface, cannot be rigid at their base and must detect orientation changes.

The mechanisms for establishing the cross-sectional shape of these extensions are different in these two systems. In maturing hairs, the pimples located near the base of the inferior surface are activated. This event is responsible for generating actin bundles that contribute to the rose thorn shape of each hair. In short, the direction of each hair and its short stocky shape is frozen by this asymmetry coupled to the early formation of an exoskeleton that hardens gradually thereafter. In contrast to be mechanoreceptors, bristles with their attached dendrites must be able to rotate at their base. In essence the bristle extension and its surrounding socket cell are part of a ball and socket joint. To accommodate this motion bristles are not rose thorn–shaped but essentially cylindrical.

This study highlights the differences in actin bundle assembly that shape thoracic bristles and wing hairs in *Drosophila*. Yet what controls bundle assembly is key to this process and this control could be exerted in several ways. For example, assembly outcome could be controlled by an external signal. This seems less likely in the case of bristles and hairs because both cells utilize largely the same collection of molecules involved in planar cell polarity (Tree et al., 2002). There may also be a critical component unique to each structure that when present dictates the specific assembly pathway. For example, membrane-tethered myosin molecules may anchor filaments in such a way as to facilitate their cross-bridging into stable longitudinal bundles. In this respect, stereocilium length is controlled in part by myosin molecules (reviewed in Frolenkov *et al.*, 2004). Finally, the relative proportions of key components early in assembly may push the assembly down one pathway versus another. For example, high concentrations of fascin may increase the survival of filaments against the always-present tide of turnover in the cell. Coupled with an actin-membrane linker, this may lead to longer and/or thicker bundles. Careful examination of the bristle and hair cytoskeleton assembly may prove fruitful in answering these questions.

ACKNOWLEDGMENTS

We thank Jeff Axelrod, Vladislav Verkhusha, Nancy Petersen, and the Drosophila Stock Center (Bloomington, IN) for generously providing fly stocks and to the Developmental Studies Hybridoma Bank (University of Iowa) for generously making available monoclonal antibody reagents. This work was supported by grants from the National Science Foundation to G.M.G. (MCB-0344136) and from the National Institutes of Health to L.G.T. (GM-52857).

REFERENCES

Adler, P. N. (2002). Planar signaling and morphogenesis in *Drosophila.* Dev. Cell *2*, 525–535.

Bainbridge, S. P., and Bownes, M. (1981). Staging the metamorphosis of *Drosophila melanogaster.* J. Embryol. Exp. Morphol. *66*, 57–80.

Brand, A. H., and Perrimon, N. (1993). Targeted gene expression as a means of altering cell fates and generating dominant phenotypes. Development *118*, 401–415.

Cant, K., Knowles, B. A., Mooseker, M. S., and Cooley, L. (1994). *Drosophila* singed, a fascin homolog, is required for actin bundle formation during oogenesis and bristle extension. J. Cell Biol. *125*, 369–380.

Drysdale, R. A., Crosby, M. A., and The Flybase Consortium. (2005). Flybase: genes and gene models. Nucleic Acids Res. *33*, D390–D395. http://flybase.org.

Eaton, S., Wepf, R., and Simons, K. (1996). Roles for Rac1 and Cdc42 in planar polarization and hair outgrowth in the wing of *Drosophila.* J. Cell Biol. *135*, 1277–1289.

Fristrom, D., and Fristrom, J. W. (1993). The metamorphic development of the adult epidermis. In: The Development of *Drosophila melanogaster*, Cold Spring Harbor, NY: Cold Spring Harbor Press, 843–897.

Frolenkov, G. I., Belyantseva, I. A., Friedman, T. B., and Griffith, A. J. (2004). Genetic insights into the morphogenesis of inner ear hair cells. Nat. Rev. Genet. *5*, 489–498.

Guild, G. M., Connelly, P. S., Ruggiero, L., Vranich, K. A., and Tilney, L. G. (2003). Long continuous actin bundles in *Drosophila* bristles are constructed by overlapping short filaments. J. Cell Biol. *162*, 1069–1077.

Guild, G. M., Connelly, P. S., Vranich, K. A., Shaw, M. K., and Tilney, L. G. (2002). Actin filament turnover removes bundles from *Drosophila* bristle cells. J. Cell Sci. *115*, 641–653.

Johnson, R. L., Grenier, J. K., and Scott, M. P. (1995). Patched overexpression alters wing disc size and pattern: transcriptional and post-transcriptional effects on hedgehog targets. Development *121*, 4161–4170.

Lawrence, P. A., Casal, J., and Struhl, G. (2002). Towards a model of the organisation of planar polarity and pattern in the *Drosophila* abdomen. Development *129*, 2749–2760.

Lawrence, P. A., Johnston, P., and Morata, G. (1986). *Drosophila*: a practical approach. Chapter *10*, Methods of Marking Cells, Oxford: IRL Press Limited.

Lees, A. D., and Picken, L.E.R. (1944). Shape in relation to fine structure in the bristles of *Drosophila melanogaster*. Proc. Roy. Soc. London Ser. B Biol. Sci. *132*, 396–423.

Lindsley, D. L., and Zimm, G. G. (1992). The Genome of *Drosophila melanogaster*, San Diego: Academic Press.

Mahajan-Miklos, S., and Cooley, L. (1994). The villin-like protein encoded by the *Drosophila* quail gene is required for actin bundle assembly during oogenesis. Cell *78*, 291–301.

Mitchell, H. K., Edens, J., and Petersen, N. S. (1990). Stages of cell hair construction in *Drosophila.* Dev. Genet *11*, 133–140.

Mitchell, H. K., Roach, J., and Petersen, N. S. (1983). The morphogenesis of cell hairs on *Drosophila* wings. Dev. Biol. *95*, 387–398.

Petersen, N. S., Lankenau, D. H., Mitchell, H. K., Young, P., and Corces, V. G. (1994). Forked proteins are components of fiber bundles present in developing bristles of *Drosophila melanogaster.* Genetics *136*, 173–182.

Tilney, L. G., Connelly, P., Smith, S., and Guild, G. M. (1996). F-actin bundles in *Drosophila* bristles are assembled from modules composed of short filaments. J. Cell Biol. *135*, 1291–1308.

Tilney, L. G., Connelly, P. S., Ruggiero, L., Vranich, K. A., and Guild, G. M. (2003). Actin filament turnover regulated by cross-linking accounts for the size, shape, location, and number of actin bundles in *Drosophila* bristles. Mol. Biol. Cell *14*, 3953–3966.

Tilney, L. G., Connelly, P. S., Ruggiero, L., Vranich, K. A., Guild, G. M., and Derosier, D. (2004). The role actin filaments play in providing the characteristic curved form of *Drosophila* bristles. Mol. Biol. Cell *15*, 5481–5491.

Tilney, L. G., Connelly, P. S., Vranich, K. A., Shaw, M. K., and Guild, G. M. (1998). Why are two different cross-linkers necessary for actin bundle formation in vivo and what does each cross-link contribute? J. Cell Biol. *143*, 121–133.

Tilney, L. G., Connelly, P. S., Vranich, K. A., Shaw, M. K., and Guild, G. M. (2000a). Actin filaments and microtubules play different roles during bristle elongation in *Drosophila*. J. Cell Sci. *113*, 1255–1265.

Tilney, L. G., Connelly, P. S., Vranich, K. A., Shaw, M. K., and Guild, G. M. (2000b). Regulation of actin filament cross-linking and bundle shape in *Drosophila* bristles. J. Cell Biol. *148*, 87–100.

Tilney, L. G., Tilney, M. S., and Guild, G. M. (1995). F actin bundles in *Drosophila* bristles. I. Two filament cross-links are involved in bundling. J. Cell Biol. *130*, 629–638.

Tree, D. R., Ma, D., and Axelrod, J. D. (2002). A three-tiered mechanism for regulation of planar cell polarity. Semin. Cell Dev. Biol. *13*, 217–224.

Turner, C. M., and Adler, P. N. (1995). Morphogenesis of *Drosophila* pupal wings in vitro. Mech. Dev. *52*, 247–255.

Turner, C. M., and Adler, P. N. (1998). Distinct roles for the actin and microtubule cytoskeletons in the morphogenesis of epidermal hairs during wing development in *Drosophila*. Mech. Dev. *70*, 181–192.

Verkhusha, V. V., Tsukita, S., and Oda, H. (1999). Actin dynamics in lamellipodia of migrating border cells in the *Drosophila* ovary revealed by a GFP-actin fusion protein. FEBS Lett. *445*, 395–401.

Wong, L. L., and Adler, P. N. (1993). Tissue polarity genes of *Drosophila* regulate the subcellular location for prehair initiation in pupal wing cells. J. Cell Biol. *123*, 209–221.